International Journal of Pharmaceutics

Nasal powders of quercetin-β-cyclodextrin derivatives complexes with mannitol/lecithin microparticles for Nose-to-Brain delivery: In vitro and ex vivo evaluation

--Manuscript Draft--

Manuscript Number:	
Article Type:	Research Paper
Section/Category:	
Keywords:	Quercetin; nasal powder; Alzheimer's disease; β-cyclodextrin derivatives; ex vivo nasal permeability; nose-to-brain delivery
Corresponding Author:	Georgia Valsami, PhD National and Kapodistrian University of Athens Athens, GREECE
First Author:	Paraskevi Papakyriakopoulou, Bachelor of Pharmacy
Order of Authors:	Paraskevi Papakyriakopoulou, Bachelor of Pharmacy
	Konstantina Manta, Bachelor of Pharmacy
	Christina Kostantini, Msc
	Stefanos Kikionis, PhD
	Sabrina Banella, Bachelor of Pharmacy
	Efstathia Ioannou, PhD
	Eirini Christodoulou, PhD
	Dimitrios M. Rekkas, PhD
	Paraskevas Dallas, PhD
	Maria Vertzoni, PhD
	Georgia Valsami, PhD
	Gaia Colombo, PhD
Abstract:	Quercetin, a flavonoid with possible neuroprotective action has been recently suggested for the early-stage treatment of Alzheimer's disease. The low solubility and extended first pass effect render quercetin unsuitable for oral administration. Alternatively, brain targeting is more feasible with nasal delivery, by-passing, non-invasively, Blood Brain Barrier and ensuring rapid onset of action. Aiming to increase quercetin's disposition into brain, nasal powders consisting of quercetin-Cyclodextrins (methyl-β-cyclodextrin and hydroxypropyl-β-cyclodextrin) lyophilizates blended with spray-dried microparticles of mannitol/lecithin were prepared. Quercetin's solubility at 37 o C and pH 7.4 was increased 19-35 times when complexed with cyclodextrins. Blending lyophilizates in various ratios with mannitol/lecithin microparticles, results in powders with improved morphological characteristics as observed by X-ray Diffraction and Scanning Electron Microscopy analysis. In vitro characterization of these powders using Franz cells, revealed rapid dissolution and permeation 17 (methyl-β-cyclodextrin) to 48 (hydroxypropyl-β-cyclodextrin) times higher than that of pure quercetin. Ex vivo powders' transport across rabbit nasal mucosa was found more efficient in comparison with the pure Que. The overall better performance of quercetin-hydroxypropyl-β-cyclodextrin powders is confirmed by ex vivo experiments revealing amount of quercetin permeated ranging from 0.03±0.01 to 0.22±0.05 for hydroxypropyl-β-cyclodextrin and 0.022±0.01 to 0.17±0.04 for methyl-β-cyclodextrin powders, while the permeation of pure quercetin was negligible.
Suggested Reviewers:	Francesco Trotta, PhD Professor, Università degli Studi di Torino: Universita degli Studi di Torino francesco.trotta@unito.it For his extensive work on the use of cyclodextrins in drug delivery

	Erem Bilensoy, PhD Professor, Hacettepe University: Hacettepe Universitesi erremino@hacettepe.edu.tr For her extensive work on the use of cyclodextrins in pharmaceutics cosmetics and biomedicine.
	Sophia Antimisiaris, PhD Professor, University of Patras: Panepistemio Patron santimis@upatras.gr For her extensive work on drug delivery systems for brain targeting
	Rita Ambrus, PhD Assistant Professor, University of Szeged: Szegedi Tudomanyegyetem arita@pharm.u-szeged.hu For her work on cyclodextrins and nasal delivery

Research Paper

Nasal powders of quercetin-β-cyclodextrin derivatives complexes with mannitol/lecithin microparticles for Nose-to-Brain delivery: *In vitro* and *ex vivo* evaluation

Paraskevi Papakyriakopoulou[1], Konstantina Manta[1], Christina Kostantini[1], Stefanos Kikionis[2], Sabrina Banella[3], Efstathia Ioannou[2], Eirini Christodoulou[1], Dimitrios M. Rekkas[1], Paraskevas Dallas[1], Maria Vertzoni[1], Georgia Valsami[1,*], Gaia Colombo[3]

1. Section of Pharmaceutical Technology, Department of Pharmacy, School of Health Sciences, National and Kapodistrian University of Athens, 15784, Greece
2. Section of Pharmacognosy and Chemistry of Natural Products, Department of Pharmacy, School of Health Sciences, National and Kapodistrian University of Athens, 15784, Greece
3. Department of Life Sciences and Biotechnology, University of Ferrara, 44121, Italy

*Corresponding author:
Professor Georgia Valsami,
Department of Pharmacy, School of Health Sciences,
National and Kapodistrian University of Athens,
Panepistimiopolis, 15784 Zografou, Greece
Tel. +30 210 727 4022
Email: valsami@pharm.uoa.gr

Abbreviation list:

AD: Alzheimer Disease; APIs: Active Pharmaceutical Ingredients; BBB: Blood Brain Barrier; CD: Cyclodextrin; CNS: Central Nervous System; F: Formulation; HP-β-CD: Hydroxypropyl-β -cyclodextrin; Me-β-CD: Methyl-β -cyclodextrin; MLMPs: Microparticles of mannitol/lecithin; NA: Nasal Administration; Que: Quercetin; Que-HP-β-CD: Quercetin- hydroxypropyl-β -cyclodextrin; Que-Me-β-CD: Quercetin- methyl-β -cyclodextrin; SEM: Scanning Electron Microscopy; UWL: Unstirred Water Layer ; XRD: X-ray Diffraction

ABSTRACT

Quercetin, a flavonoid with possible neuroprotective action has been recently suggested for the early-stage treatment of Alzheimer's disease. The low solubility and extended first pass effect render quercetin unsuitable for oral administration. Alternatively, brain targeting is more feasible with nasal delivery, by-passing, non-invasively, Blood Brain Barrier and ensuring rapid onset of action. Aiming to increase quercetin's disposition into brain, nasal powders consisting of quercetin-Cyclodextrins (methyl-β-cyclodextrin and hydroxypropyl-β-cyclodextrin) lyophilizates blended with spray-dried microparticles of mannitol/lecithin were prepared. Quercetin's solubility at 37^{o}C and pH 7.4 was increased 19-35 times when complexed with cyclodextrins. Blending lyophilizates in various ratios with mannitol/lecithin microparticles, results in powders with improved morphological characteristics as observed by X-ray Diffraction and Scanning Electron Microscopy analysis. *In vitro* characterization of these powders using Franz cells, revealed rapid dissolution and permeation 17 (methyl-β-cyclodextrin) to 48 (hydroxypropyl-β-cyclodextrin) times higher than that of pure quercetin. *Ex vivo* powders' transport across rabbit nasal mucosa was found more efficient in comparison with the pure Que. The overall better performance of quercetin-hydroxypropyl-β-cyclodextrin powders is confirmed by *ex vivo* experiments revealing amount of quercetin permeated ranging from 0.03±0.01 to 0.22±0.05 for hydroxypropyl-β-cyclodextrin and 0.022±0.01 to 0.17±0.04 for methyl-β-cyclodextrin powders, while the permeation of pure quercetin was negligible.

KEYWORDS: Quercetin; nasal powder; Alzheimer's disease; β-cyclodextrin derivatives; *ex vivo* nasal permeability; nose-to-brain delivery

1.Introduction

Alzheimer's disease (AD) is a neurodegenerative disease that causes severe dementia and memory loss. According to the Alzheimer's Association report in 2017, AD is considered the 6th leading cause of death [1]. AD is one of the major Central Nervous System (CNS) diseases occurring in adults and although it usually affects elderly people, modern lifestyles have led to the onset of the disease at younger ages. The disease is characterized by gradual degeneration of neurons, which leads to loss of cognitive ability, memory impairment and in many cases, dysfunction in the daily activities [2]. The exact cause of the disease has not been determined yet, but genetic factors, eating habits and mental stress seem to contribute to its occurrence. The main hypotheses for the development of AD include a) the hypothesis of β-amyloid accumulation, b) the Tau hypothesis, c) the cholinergic hypothesis, d) the hypothesis of stimulatory toxicity and e) the hypothesis of mitochondrial cascade. Oxidative stress is strongly associated with all the mentioned hypotheses as a major factor for the onset and the progression of AD [3,4].

According to the hypothesis of β-amyloid accumulation, the increased concentration of β-amyloid plaques in neurons results in toxicity, expressed as neuroinflammation [5]. Restraining of this neuroinflammation seems to be a possible therapeutic goal for the treatment of AD. Several studies support that a diet based on food rich in polyphenols, as well as the consumption of food supplements containing specific polyphenolic derivatives, exerts a beneficial effect on health. The neuroprotective effect of polyphenols has been extensively studied, considering the benefits of their administration in cases of neurodegenerative diseases [6].

A widely studied phenolic derivative quercetin (Que), is a flavonoid associated with a possible neuroprotective activity that reduces oxidative stress when administered *in vivo* [7]. The contribution of oxidative stress to the occurrence of AD is the basis of the possible therapeutic effect of Que. More specifically, lipid peroxidation appears to destroy the lipid membranes of the brain, which seems to lead to neurodegenerative diseases such as AD [8]. Que's ability to scavenge free radicals is attributed to its catechol hydroxyl groups. Also, both the complexation of iron and calcium and the inhibition of lipid peroxidation contribute to its effectiveness against oxidative stress [9]. In particular, Que appears to have, in addition to its antioxidant activity, an ability to improve cholinergic function and thus, it is considered as a possible additional neuroprotective effect. However, Que's action is limited due to both its low absorption by the gastrointestinal tract and its difficulty in crossing the blood-brain barrier (BBB) [10].

The oral route is the most used mode of administration in order to achieve therapeutic levels of a drug in the bloodstream. However, most of the Active Pharmaceutical Ingredients (APIs) exhibit low oral bioavailability, due to their low aqueous solubility, degradation in the gastrointestinal tract and/or extensive first pass metabolism. In the last decade, many studies focused on alternative routes of drug delivery in order to overcome oral administration constrains [8,9]. More specifically, regarding the neuronal targets, orally administered APIs usually have limited access to the CNS, due to the presence of the BBB. This results in the reduced efficacy of the drugs in CNS diseases [13].

Nasal Administration (NA) has been mainly used for the local treatment of chronic diseases, such as chronic rhinosinusitis, nasal congestion, rhinorrhea and nasal cavity infections [14]. Nasal delivery is a non-invasive route of administration, which has many advantages, including the ease of administration, patient's compliance, rapid onset of action, adequate permeability and absorption area, reduced enzymatic activity and avoidance of first pass effect. Moreover, through the olfactory region of the nose, the drug could be absorbed by-passing the BBB. In the last decade, all these benefits have built a trend towards the development of nasal administered formulations for CNS diseases [15].

In order for a compound to be considered for intranasal delivery, many factors must be determined and especially, its permeability through the nasal mucosa [16-18]. In addition, it is important to study new strategies for permeability enhancement and test the extent of toxicity that may be caused from repeated administrations into the nose [19]. Cyclodextrins (CDs) have been extensively considered as nasal excipients due to their ability to solubilize lipophilic drugs or drugs with low aqueous solubility [20]. They can also enhance drug absorption of hydrophilic or water-soluble drugs as a result of their capacity to form complexes with membrane components, mainly lipids, which cause not only disruption of the nasal barrier but also may change the elasticity of the nasal mucosa [21]. Very recently, a nasal powder of glucagon, containing only β-cyclodextrin as the sole excipient, has been marketed [22].

In a previous study we investigated lyophilized compositions of quercetin with methyl-β-cyclodextrin and hydroxypropyl-β-cyclodextrin (Que-Me-β-CD and Que-HP-β-CD, respectively) [23], which significantly improved Que's solubility in water and enabled its diffusion *ex vivo*, across rabbit nasal mucosa. The aim of the present research was the preparation of nasal powders, composed of the Que-CDs lyophilizates blended with spray-dried microparticles of mannitol/lecithin (MLMPs), for treating AD neuroinflammation [24-25]. X-ray Diffraction (XRD) and Scanning Electron Microscopy (SEM) analyses were performed

to determine the blends' morphology. Nasal powders were characterized *in vitro* and *ex vivo*, to investigate the possible interactions of MLMPs with Que-CDs and more in particular the contribution of MLMPs to the morphological and biopharmaceutical characteristics of the nasal powders.

2. Materials and Methods

2.1. Chemicals and Reagents

Quercetin (MW 302.24 g/mol), methyl-β-cyclodextrin (Me-β-CD; MW 1310 g/mol), hydroxypropyl-β-cyclodextrin (HP-β-CD; MW 1460 g/mol) were purchased from Sigma-Aldrich (St Louis, MO, USA), Fluka Chemika (Mexico City, Mexico US & Canada) and Ashland (Covington, KY, USA), respectively. Mannitol (Ph. Eur.) was supplied by Lisapharma S.p.A. (Erba, Italy) and soybean lecithin (Lipoid® S45) by Lipoid AG (Steinhausen, Switzerland). Regenerated cellulose membranes (MW cut-off 5000 Da, diameter 63 nm) were obtained from Dia-norm GmbH (Berlin, Germany). HPLC grade solvents and reagents were obtained from Merck (Darmstadt, Germany) and Fischer Scientific (Pittsburgh, PA, USA). Triple-deionized water from Fischer Scientific was used for all preparations.

2.2. Preparation of Que-CD Complexes

Lyophilized powders of Que-Me-β-CD and Que-HP-β-CD were prepared by freeze-drying aqueous solutions of Que-Me-β-CD and Que-HP-β-CD, as previously described [23], in molar ratio of 1:1 and 1:2, respectively. Briefly, 2.17 g of Me-β-CD or 4.8 g of HP-β-CD were transferred in a 600 mL beaker and suspended with 500 mL of water. Subsequently, 500 mg of Que were added under continuous stirring and light protection (due to the photosensitivity of Que), followed by the addition of small amounts of ammonium hydroxide 6% (v/v) until the complete dissolution of Que, while pH was continuously monitored and adjusted to approximately 9.0-9.5. The solution obtained was transferred into round trays for lyophilization, frozen at -73 °C and freeze-dried using Vacuum Freeze Dryer [BK-FD10T, Biobase biodustry (Shandong) CO., LTD (China)]. Que's content was quantified in both lyophilized powders by high pressure liquid chromatography (HPLC) [Section 2.9].

2.3. Preparation of Spray-Dried MLMPs

MLMPs were prepared by spray drying an ethanolic feed solution of mannitol/lecithin (ratio 92:8 w/w) according to Balducci et al. [18]. The final solution contained 8% (v/v) of ethanol and 2% (w/v) solid content. The solution was spray-dried on a Mini Spray Dryer B-191 (BÜCHI

Labortechnik AG , Flawil, Switzerland) at a flow rate of 6.5 mL/min, inlet temperature of 100 °C, aspiration 100%, and air flow of 600 NL h^{-1} [18]. The spray-dried mannitol/lecithin powder was used to prepare the blends with the Que-Me-β-CD and Que-HP-β-CD complexes. The % yield of the spray drying process applied, was calculated as the ratio of the mass of recovered microparticles over the initial mass of total solids dissolved in the feed solution.

2.4. Preparation of Blends

Blends of spray-dried MLMPs powder with Que-Me-β-CD and Que-HP-β-CD lyophilized powders, respectively, were prepared manually in a glass vial with a spatula in different ratios (MPLPs/Que lyophilized powder ratios: 25:75, 50:50, 75:25). The time of mixing for each preparation was 20 min. Determination of Que's content was carried out by HPLC analysis under the conditions described in Section 2.9.

2.5. X-Ray Diffraction (XRD) Analysis

The X-Ray diffractograms were obtained using a Bruker D8 Advance XRD apparatus (Bruker AXS GmbH, Karlsruhe, Germany) equipped with a Copper anode tube at a voltage of 40 kV and 25 mA. The scanned angles (2θ) were between 5° and 70° with an increment size of 0.02° at 0.5 sec/step. The analysis was carried out at room temperature. Poly Methyl Meth Acrylate (PMMA) sample holders with a capacity of ≈ 300 mg were used for obtaining all X-Ray diffractograms.

2.6. Scanning Electron Microscope (SEM) analysis

A PhenomWorld desktop scanning electron microscope (SEM, Thermo Fischer Scientific, Waltham, MA, USA) with a tungsten filament (10 kV) and charge reduction sample holder was employed for the SEM analyses of the raw materials and the formulations.

2.7. *In vitro* diffusion experiments

In vitro diffusion experiments were carried out using regenerated cellulose membranes with a molecular cut-off of 5000 Da and Franz-type diffusion cells (Crown Glass, Somerville, MA, USA). The membranes were prepared with immersion in distilled water for 15 min. After replacing water with fresh volume, the membranes were allowed to soak in it for 30 more min. Then, they were transferred to a beaker with Phosphate Buffer Solution (PBS, pH 7.4), where they remained soaked for 15 min. After this pre-treatment, the membranes were cut into squares of 1 cm^2 surface in order to cover completely the Franz cells' diffusion area (0.636 cm^2). The Franz cells were assembled filling the receptor compartment with 5 mL of PBSand

177 the membrane was mounted between the receptor and donor compartments. A magnetic
178 stirrer was added in the receptor and the two parts were kept together with a metal clamp.
179 The assembled system was allowed to equilibrate at 37 °C for 15 min. Then, 25 mg of each
180 test formulation (Table 1) or 15 mg of pure Que were placed in the donor compartment and
181 wet with 100 μL of PBS. The donor and receptor compartments were both covered with
182 Parafilm® to prevent evaporation. All experiments lasted for 2 h. At specific time intervals, 0.5
183 mL were sampled from the receptor compartment and replaced by an equal volume of fresh
184 PBS. The samples were analyzed by an HPLC method [see 2.9]. At the end of the experiment,
185 the residual formulation in the donor compartment was quantitatively collected and diluted
186 in order to determine the remaining Que and calculate the mass balance. The cellulose
187 membranes were washed with H_2O/methanol (50:50) solution, to retrieve the amount of Que
188 remaining in the membrane and the extract was also quantified by HPLC [see section 2.9].

189 2.8. *Ex vivo* diffusion experiments

190 Rabbit nasal mucosa was selected for the *ex vivo* diffusion experiments. Nasal mucosa was
191 extracted on the day of the experiment from rabbit heads collected from a local
192 slaughterhouse (Finale Emilia, Italy and Athens, Greece). More precisely, to isolate the
193 mucosa, a surgical scissor was used in order to cut each nostril in two places on either side of
194 the septum. Ethmoidal air cells were removed with surgical forceps and the parts around the
195 septum were cleaned carefully. Then, the teeth were removed from both sides. The nose bone
196 was cut vertically at the end of the diaphragm (next to the eyes) with the surgical scissors, and
197 the diaphragm was removed. The mucosa was gently isolated from both sides of the septum
198 using a spatula. During the isolation, the mucosa was maintained hydrated with saline
199 solution. After mucosa's extraction, the Franz cells' receptor compartment was filled with PBS
200 (pH 7.4) and magnetic stirring bar was also added. The extracted mucosa was mounted
201 between the donor and receptor compartments of Franz diffusion cell, with the mucosal side
202 facing the donor. In order to assess the proper cell assembly and the integrity of the mucosa,
203 the donor compartment was filled with saline solution, checking that no liquid passed to the
204 empty receptor due to inappropriate mounting or lack of tissue integrity. Cell equilibration,
205 formulation loading into the donor, sampling and recovering of residual Que from the donor,
206 is described in section 2.5. The drug accumulated in the tissue was recovered by comminuting
207 the mucosa with a surgical blade and homogenizing with a small pestle or Ultra-Turrax® IKA
208 (T10 basic model, IKA®-Werke GmbH & Co. KG, Staufen, Germany), three times, using 300 μL
209 of water for 30 sec each time. Then, it was further homogenized with 300 μL of acetonitrile
210 for 30 sec. After homogenization, the extract was diluted and centrifuged before HPLC

analysis. Que's amounts recovered from the mucosa, receptor and donor compartments allowed for the calculation of the mass balance.

2.9. HPLC method

HPLC analysis was performed on a Shimadzu prominence system composed of a LC-20AD Quaternary Gradient Pump with degasser, with a SIL-HT auto-sampler and a photo-diode array detector SPD-M20A. Data acquisition and analysis were performed by LC solution® software. Analysis was carried out on an analytical reverse phase Thermo Aquasil C_{18} column (150×4.6 mm, 5 µm particle size) connected to a C18 precolumn (12.5×4.6 mm, 5 µm particle size), using water:acetonitrile (65:35 v/v) as the mobile phase, at 1 ml/min flow rate. The injection volume was 20 µL. The method of Sanghavi' s et al. [26] was optimized for the needs of the present work and the calibration curve samples range from 5 to 100 µg/mL of Que. The calibration curve samples were prepared using appropriate volumes of Que's methanolic stock solution (1 mg/mL) and mobile phase (H_2O/ Acetonitrile, 65:35) for all dilutions.

2.10. Statistical analysis

Data distribution was tested using the Shapiro-Wilk (S-W) normality test. Significance was set at $p < 0.05$ level and all tests were two-tailed with 95% Confidence Intervals (CI). Results are expressed as mean ± standard deviation (SD) for the *in vitro* diffusion experiments and mean ± standard error (SE) for *ex vivo* experiments. Permeation values were statistically compared between the different formulations and per time point within the formulation. Outlier detection occurred applying the Interquartile Range (IQR) using a step of 1.5 x IQR. No outliers were detected. The Shapiro-Wilk test results revealed that the parameter sets for *in vitro* experiments could be considered as Gaussian distributed. Consequently, parametric statistics were applied to confirm whether the differences observed between the compared groups (e.g., different formulations) were statistically significant or not. One-way ANOVA was performed on the obtained values (normally distributed) to detect possible statistically significant differences between the compared groups. Non-parametric tests were applied in case of *ex vivo* experiments, because the parameter sets could not be considered as Gaussian distributed. Kruskal-Wallis was performed to statistically evaluate the differences between the formulations at every time point of the experiment and post-hoc Mann-Whitney to detect individual differences. Data analysis was performed using SPSS version 26.0 (IBM SPSS Statistics for Windows, Version 26.0, IBM Corporation, Armonk, NY, USA) software package.

3.Results

3.1. Que's content in the blends

Eight formulations (F1-F8, Table 1) composed of Que-Me-β-CD or Que-HP-β-CD and MLMPs in different ratios were prepared and characterized in the present study. Que-CD complexes and spray-dried microparticles with excipients, were obtained in yields which were found in line with previous works [23,27]. More in particular, the microparticles were collected with a yield of 54.5%. The amount of Que in the blend formulations of Que-Me-β-CD ranged from 3.0% to 12.4% (w/w), whereas using Que-HP-β-CD it ranged from 1.8% to 7.3% (w/w) (Table 1). Based on these values, the amount of Que in 25 mg of each Formulation (F) used for the diffusion experiments was calculated and is reported in Table 1.

3.2. X-Ray Diffraction (XRD) Analysis

The X-Ray diffractograms of formulations F1-F4 in comparison with the diffractograms of Que and MLMPs are presented in Figure 1A, while the comparison of the diffractograms of formulations F5-F8 with Que and MLMPs are presented in Figure 1B. Que as a raw material exhibits many distinct sharp peaks over a 2θ range of 5-30° with a very strong sharp diffraction peak at 12.879°, revealing a crystalline structure. These data are in line with data obtained by Dian et al. [28]. The XRD pattern of Me-β-CD and HP-β-CD showed two broad peaks in the ranges of 8–15° and 15–22° (2θ), confirming the amorphous nature of both CD (Figures 1A, B). Total disappearance of crystalline Que characteristic peaks was observed in both Que-CD complexes (F1 and F5), indicating the transition of the compound from a crystalline to an amorphous state due to the lyophilization process. The spray - dried MLMPs are present in a crystalline form based on the peaks observed in their X-Ray diffractograms (Figure 1A, B). The X-Ray diffractograms of the formulations containing mannitol/lecithin (F2-F4 and F5-F7), showed approximate superimposition of the individual patterns of mannitol/lecithin and, Que was present in the amorphous state in all blends (lack of Que peak at 2θ of 12.879°).

3.3. Scanning Electron Microscope (SEM) analysis

SEM analyses were performed to investigate the morphological changes that occur upon blending of the lyophilized powders with the MLMPs. SEM analysis was also carried out for the raw materials (Que, MLMPs, Me-β-CD and HP-β-CD) used for the preparation of the blends (Figure 2). It is well known that the lyophilization process favors the formation of amorphous solids after the sublimation of water from the frozen solutions. SEM micrographs indicated that the prepared lyophilized powders of Que-Me-β-CD and Que-HP-β-CD complexes

(formulations F1 and F5, respectively), in contrast to the raw materials (Figure 2A-D), were in the form of flake-like particles randomly distributed in irregular shapes of various sizes (Figure 2E, Figure 2I). These results were in line with the ones reported in the literature [29,30]. For both complexes, after 20 min blending of the lyophilized powders with the MLMPs in different proportions, it was observed that the flakes were smashed in smaller pieces covered by the MLMPs (Figure 2F-2H, Figure 2J-2L). In all cases, the microparticles were spread on the flake surfaces, exhibiting an aggregate formation with the smaller particles attached to the larger ones. In the formulations F2 and F6 containing 25% of the MLMPs, the flakes of the lyophilized powders were partially covered (Figure 2F, Figure 2J), while the sheathing became more intense as the percentage of MLMPs increased up to 50% in the F3 and F7 formulations (Figure 3G, Figure 3K). In the formulations of F4 and F8 containing 75% of the MLMPs, the flakes were almost completely covered by the microparticles (Figure 2H, Figure 2L).

3.4. *In vitro* diffusion experiments

In order to evaluate the diffusion/release behavior of the lyophilized Que-CDs powders and the prepared formulations after blending with different amounts of MLMPs, Que diffusion through regenerated cellulose membranes was studied using Franz cells. Since it was decided to load the same powder amount, this led to different loaded “doses” of Que. Thus, total transported Que data are expressed as percentage of the loading dose to compare the different formulations. As observed in Figure 3 A,B, both Que-Me-β-CD and Que-HP-β-CD lyophilized powders and their blends with MLMPs presented a better diffusion profile through the artificial membrane, as compared to pure Que ($p < 0.05$, 95% CI). More precisely, the % permeated amount across the artificial membrane was 17 to 48 times higher in the case of blends than pure Que, at all time points. Also, the permeation of formulations containing HP-β-CD (Figure 3B) was twice higher compared with the ones containing Me-β-CD (Figure 3A). Regarding the formulations with Me-β-CD (Figure 3A), F1, F2 and F4, they all resulted in similar amounts permeated at all time points expressed as % of loading dose ($p > 0.05$, 95% CI), while F3 seems to promote permeation more during the 1st hour only. However, during the second hour the four formulations exhibited the same permeation pattern. The % of loading dose permeated vs time for the formulations containing HP-β-CD (Figure 3B) did not differ significantly between each other, but it should be noted that a trend for higher permeation with increasing MLMPs amount in the formulation was observed at later time points (90-120 min). The lowest % value was observed with pure Que, which was achieved in the first time point (15 min) and remained constant thereafter.

All formulations reached a plateau after a maximum of 90 min. As the rate- limiting step for Que to permeate through the cellulose membrane is its aqueous solubility, the presence of plateau indicates that diffusion is stopped likely after an equilibrium concentration between receptor and donor compartments was reached. This plateau is more evident for formulations F1-F4, containing Me-β-CD, compared to formulations F5-F8 containing HP-β-CD ($p>0.05$, 95% CI). The 1:2 molar ratio (Que:HP-β-CD) of the complex with the more hydrophilic β-CD derivative (HP-β-CD) in F5-F8, compared to the 1:1 molar ratio when using the less hydrophilic Me-β-CD in F1-F4, could be the reason of the early plateau of the latter. In fact, the lyophilized complex of Que-HP-β-CD was found freely soluble at pH 7.4, 37 °C as compared to Que-Me-β-CD complex (see Supplementary Material).

The results as shown in the cumulative amount graph (Figure 4) revealed that, the lyophilized Que-CD powders (F1 and F5) presented the highest permeations in terms of total amount of Que permeated per unit area (0.19 ± 0.02 and 0.24 ± 0.03 mg/cm^2, respectively), at the 2 h time point . Comparing the performance of the two lyophilized products, F1 and F5, it is evident that Que permeation in F5, containing HP-β-CD, is higher than that of F1, containing Me-β-CD.

Overall, as shown in Figure 4, the presence of MLMPs decreased the amount of Que permeated per unit area at all tested ratios (Table 1), in comparison to the pure lyophilized powder. This is rather expected, since, as the amount of Que decreases, the available diffusion surface area decreases as well. Especially, in the case of F4 [Que-Me-β-CD:MLMPs (25:75)] the permeated amount of Que is equal to that of pure Que. The similar permeation between F4 and pure Que could also be interpreted taking into account the 20-fold higher loading with pure Que than F4 (15 mg vs. 0.74 mg).

Considering the effect of CD on Que permeation through cellulose membranes, the results depicted in Figure 4 show that among blends containing the same amount of MLMPs (F2-F6; F3-F7; F4-F8), those with HP-β-CD result in higher Que amount permeated per unit area.

3.5. *Ex vivo* diffusion experiments

The percentages of Que transported across rabbit nasal mucosa at different time points are presented in Figure 5 A, B. Among the formulations F1-F4 containing Me-β-CD (Figure 5A), F2 showed the highest permeation at 120 min, achieving 3.77 ± 0.64% of the loading dose, whereas F4 exhibits similar onset of permeation, then reaching a plateau of 1.26 ± 0.11% at 60 min. In the case of formulations F5-F8 containing HP-β-CD (Figure 5B, the most permeable at 120 min, seems to be the lyophilized powder of Que-HP-β-CD (F5), whose permeation reaches a value of 7.61 ± 0.72% of the loading dose, while all formulations exhibit the same

permeation rate for the first 45 min. The permeated amount of pure Que through rabbit nasal mucosa was negligible and thus it is not shown in the graph. The two formulations with the greater amount of MLMPs (F4, F8) seem to exhibit the least fraction of loading dose permeated through the nasal mucosa, within the group containing the same cyclodextrin. As the percentage of MLMPs in the formulation decreases, it was observed that in case of HP-β-CD, there are no differences in the % permeated from F5-F7 until the 90 min time point of the *ex vivo* experiment. At this time point, F6 and F7 reach a plateau, while Que permeation from F5 continues linearly for the entire 2h duration of the experiment, reaching a final value significantly greater than F6 and F7 ($p<0.05$, 95% CI). However, in case of Me-β-CD, the results presented in Figure 5A showed that the presence of MLMPs at the 25% in the formulation (F2), led to a better performance in comparison with the pure lyophilized powder (F1). The overall better performance of HP-β-CD formulations (F5-F8) is in accordance with the data obtained from the *in vitro* diffusion experiments (Figures 3 A, B).

In Figure 6, the permeation is expressed as the quantity of Que permeated per unit area. The two lyophilized powders (F1, F5), without MLMPs, gave the greatest permeation per unit area in 2 h. For all other formulations it was observed that the higher the percentage of MLMPs in the formulation, the lower the permeation per unit area through rabbit nasal mucosa is (F2>F3>F4 and F6>F7>F8). This fact could be correlated with the different loading doses of Que among the blend formulations of the same lyophilized powder. However, between the formulations containing the same proportion of MLMPs, but different CD (F1 vs F5, F2 vs F6, F3 vs F7, F4 vs F8), those with HP-β-CD performed better.

None of the formulations reached a plateau until the end of the *ex vivo* experiment ($p<0.05$, 95% CI among the different time points of the same formulation), in contrast with the respective permeation profile with artificial membranes as model barrier (Figure 4). It should be also noted that formulations F1, F3, F5, F7 and F8 exhibited a linear increase of the amount of Que permeated per unit area of rabbit nasal mucosa with time (Table 2).

4. Discussion

The development of CNS targeting drugs is greatly restricted by the fact that only a small amount of the dose administered *per os* achieves to pass the BBB and reach the pharmacological target in the brain. The nasal cavity is a well-vascularized tissue with direct neuronal connection to the brain via the olfactory neurons and thus it is considered as the most appropriate route for the administration of drugs targeting the brain, including those for AD. In order to evaluate the nasal route for nose-to-brain delivery , product optimization should be based on the following three-axes [31]: 1. Drug's appropriate positioning on the

olfactory area and not on the larger respiratory region, 2. Sufficient retention time on the nasal mucosa surface and 3. Penetration enhancement and reduction of drug metabolism in the nasal cavity. In the present study, based on the third axis, the prepared lyophilized compositions, after being characterized by using biophysical techniques [32], were blended with MLMPs and tested for *in vitro* release using artificial membranes, as well as for *ex vivo* permeability, using the rabbit nasal mucosa model barrier [18,27]. MLMPs have been previously characterized [33] and proved appropriate for the formulation of nasal powders.

For the diffusion/release experiments, artificial membranes of regenerated cellulose with a molecular weight cutoff of 5000 Da were chosen, permitting free Que, as well as its complexes with CDs to easily pass through the membranes from the donor to the receptor compartment. Also, since these membranes are stable in the pH range 3-8, they are compatible with the receptor compartment medium (pH 7.4) [34]. Hydrophilic CD derivatives, such as HP-β-CD are capable to form hydrogen bonds with the glucose molecules of cellulose. These interactions could interfere in the cellulose's structure by destroying the hydrogen bonds or leading to structural complexity, which depends on the CD concentration. Cellulose is consisted of hydrophilic monomers which can form strong hydrogen bonds with the Unstirred Water Layer (UWL), adjoining on the membrane surface from both sides (of receptor and donor compartment). These bonds, since they are stronger than the inter-water connection cause the reduction of water molecules' mobility and the UWL is arranged on membrane's surface [35]. Layer's thickness acts as part of the barrier, increasing membrane's resistance to allow molecules' permeation. From the presented *in vitro* data, it can be assumed that hydrophilic CDs derivatives favor these interactions, forming hydrogen bonds with the regenerated cellulose membrane, disturbing the UWL and enhancing the permeation that takes place more rapidly and efficiently.

The rate of drug transfer from the donor to receptor compartment, through the artificial membrane, with a defined area (A), is expressed by the following equation:

$$\frac{\mathrm{dm}}{\mathrm{dt}} = \mathrm{A\ J} = \mathrm{K\ DA}\frac{\mathrm{dC}}{\mathrm{dx}}$$

where, dm (mg) is the mass of the transferred drug, K, the partition coefficient, D (cm^2/s) is the diffusion coefficient through a membrane, dx (cm), the thickness of membrane and dC (mg/ml) is the concentration difference between the two compartments on either side of the membrane [36].

Comparing the blend formulations which contain the same proportion of lyophilized powder, but different CD derivative, it is observed that despite the greater Que loading for Me-β-CD

formulations (F1 – F4), which mathematically could lead to greater dC between the two compartments, HP-β-CD formulations (F5-F8) presented greater permeability (Figure 4). This is probably due to the greater solubilizing effect of HP-β-CD leading to the higher solubility of Que-HP-β-CD lyophilized powder observed at pH 7.4 and 37 °C (see Supplementary Material). Moreover, it can be suggested that in the case of Me-β-CD (F1-F4), which is more lipophilic, the interactions between CD and the cellulose membranes are less favored or probably not occurring at all. This hypothesis could be justified, if based on the lower permeation, which are half in comparison with the formulations of HP-β-CD at the same MLMPs/Que lyophilized powder ratio (Figures 3 A, B and 4) and the lack of differences in the permeation profiles of F1-F4, expressed as % of loading dose (Figure 3A). The presence of cyclodextrin allows a 18-50 times greater permeation than pure Que. This twofold greater permeation of QUE from the formulations F5-F8 in comparison with F1-F4 is attributed to the double CD/Que ratio in the former.

Finally, in all permeation profiles with the artificial membranes, cessation of the permeation is observed at a maximum of 90 min. Although, it seems as if the sink conditions were lost, the maximum concentration measured in the receptor compartment (0.024 mg/mL) remains well below the 10% of saturation concentration, according to the solubility study at pH 7.4 (0.46 ± 0.02 mg/mL, see Supplementary Material) [37]. Also, in the donor compartment a small amount of the dissolution medium (100 μL) have been added to dissolve quantities of Que, which vary between 0.5 and 3.1 mg. Consequently, it can be hypothesized that at the time of plateau the remaining amount of Que in the donor compartment could not be further dissolved to sustain the dC necessary for diffusion.

On the contrary, in the *ex-vivo* experiments, a decrease in the diffusion rate is observed, while formulations F1, F3, F5, F7 and F8, exhibited a linear permeation profile when expressed as Que amount permeated per unit area (Figure 6). However, it should be mentioned, that the cut-off of cellulose membranes enables the diffusion of both free and CD-complexed Que, as well as free CD, resulting to a gradual decrease of the CD amount in the donor compartment and a consequent decrease of the dissolved Que. In addition, nasal mucosa is permeated only by the free fraction of Que that is dependent on the complexation affinity between Que and CD. Also, the results in Figure 5 A,B show that from the first hour, for formulations F5-F8, the % loading dose permeated across the rabbit nasal mucosa, was higher than that of F1-F4 and this better performance is maintained until the end of the experiment. Furthermore, data shown in Figure 3 A, B and 6 prove that, both the Que loading amount and the type of CD are critical factors to determine the permeability through both artificial and rabbit mucosa

membranes. More specifically, among the formulations containing the same amount of MLMPs (F2-F6, F3-F7, F4-F8), the ones with HP-β-CD present greater permeation (expressed as amount permeated per unit area, Figures 4, 6). In addition, the solubility study at pH 7.4 indicates that the Que-HP-β-CD complex is significantly more soluble in comparison to Que-Me-β-CD. As Que is a substance with very low aqueous solubility, the rate-limiting step to achieve the greatest possible permeated amount in the receptor compartment, is the solubility in the donor compartment. This hypothesis is also confirmed by comparing Figures 4 and 6. The comparison reveals that despite the different structure of the two barriers and even if the cut-off of the artificial membrane is 10 times greater than that of the nasal mucosa barrier [35], the achieved permeated amount at 2 h is almost equal. In many studies [38,39] Que has been noted as modulator of P-glycoproteins of endothelial cells being able to activate or inhibit them in a concentration-dependent manner. Therefore, a possible inhibition of the remaining P-glycoprotein in the tissue increases the permeability, compensating for the smaller pores of the biological barrier. Hence, in the case of class II substances (highly permeable−poorly soluble), according to the Biopharmaceutics Classification System [40], regenerated cellulose artificial membranes could be considered as a satisfactory predictor of the permeation profile of the substance through the nasal mucosa barriers.

Blending with MLMPs permits the formation of powders with ease of handling and probably better positioning in the donor compartment. Hence, as it is confirmed by the SEM images, the lower permeation of F4 and F8 could be attributed to the total coverage of the complex by MLMPs. Mannitol is a water-soluble substance and could increase the water uptake of the loaded amount, resulting in a greater solubility of the formulation [41]. Nevertheless, an excessive amount of microparticles could also increase the size of complex foils, reducing dissolution rate and causing permeation to take place more slowly and less effectively.

5. Conclusions

In the present study blends consisted of lyophilized powders of Que-HP-β-CD and Que-Me-β-CD with the spray-dried MLMPs were prepared and characterized with XRD and SEM images and further evaluated *in vitro* and *ex vivo* for their permeation through artificial and biological membranes. All the permeation experiments, using both artificial membranes and rabbit nasal mucosa as biological barrier reveal the superiority of HP-β-CD over the Me-β-CD. The presence of MLMPs would lead to the formation of powder easier to handle, probably enabling better positioning of the formulation in the nasal cavity. These results are very promising and consist great evidence for effective intranasal administration of the prepared Que formulations. To

this end, *in vivo* pharmacokinetic studies in animal model are ongoing to evaluate their performance for nose-to-brain delivery and systemic absorption of Que.

Declarations of interest: none

Funding: This research did not receive any specific grant from funding agencies in the public, commercial, or not-for-profit sectors.

Acknowledgements: The authors want to acknowledge DMV Violeta Sidira for her useful advice in rabbit nasal mucosa extraction procedure.

References

1. A. Alexander, S. Saraf, Nose-to-brain drug delivery approach: a key to easily accessing the brain for the treatment of Alzheimer's disease, *Neural Regeneration Research*, 13(12), 2102-2104, (2018), doi:10.4103/1673-5374.241458.
2. J. Folch, D. Petrov, M. Ettcheto, S. Abad, E. Sánchez-López, M.L. García, J. Olloquequi, C. Beas-Zarate, C. Auladell, A. Camins, Current research therapeutic strategies for Alzheimer's disease treatment, *Neural Plasticity*, 15, (2016), doi: 10.1155/2016/8501693.
3. Y. Zhao, B. Zhao, Oxidative Stress and the Pathogenesis of Alzheimer's disease. *Oxidative Medicine and Cellular Longevity*, 1–10, (2013), doi:10.1155/2013/316523.
4. L. Cassidy, F. Fernandez, J.B. Johnson, M. Naiker, A.G. Owoola, D.A. Broszczak, Oxidative stress in Alzheimer's disease: A review on emergent natural polyphenolic therapeutics, *Complementary Therapies in Medicine*, 49:102294, (2020), doi: 10.1016/j.ctim.2019.102294.
5. J.C. Park, S.H. Han, I. Mook-Jung, Peripheral inflammatory biomarkers in Alzheimer's disease: a brief review, *BMB Reports*, 53(1):10-19, (2020), doi: 10.5483/BMBRep.2020.53.1.309.
6. A. Atlante, G. Amadoro, A. Bobba, V. Latina, Functional Foods: An Approach to Modulate Molecular Mechanisms of Alzheimer's Disease, *Cells*, 9(11):2347, (2020), doi: 10.3390/cells9112347.
7. P.C. Paula, S.G. Angelica Maria, C.H. Luis, C.G. Gloria Patricia, Preventive Effect of Quercetin in a Triple Transgenic Alzheimer's Disease Mice Model, *Molecules*, 24(12):2287, (2019), doi: 10.3390/molecules24122287.

8. G. D'Andrea, Quercetin: A flavonol with multifaceted therapeutic applications? *Fitoterapia*, 106, 256-271, (2015), doi: 10.1016/j.fitote.2015.09.018.
9. I. Morel, G. Lescoat, P. Cogrel, O. Sergent, N. Pasdeloup, P. Brissot, P. Cillard, J. Cillard, Antioxidant and iron-chelating activities of the flavonoids catechin, quercetin and diosmetin on iron-loaded rat hepatocyte cultures*, Biochemical Pharmacology,* 45, 13–19, (1993), doi: 10.1016/0006-2952(93)90371-3.
10. A. Gupta, K. Birhman, I. Raheja, S.K. Sharma, H.K. Kar, Quercetin: A wonder bioflavonoid with therapeutic potential in disease management, *Asian Pacific Journal of Tropical Disease*, 6(3), 248-252, **(**2016), doi: 10.1016/S2222-1808(15)61024-6.
11. A. Pires, A. Fortuna, G. Alves, A. Falcao, Intranasal Drug Delivery: How, Why and What for? *Journal of Pharmacy and Pharmaceutical Sciences,* 12(3), 288 – 311, (2009), doi: 10.18433/J3NC79.
12. X. Chen, F. Zhi, X. Jia, X. Zhang, R. Ambardekar, Z. Meng, A.R. Paradkar, Y. Hu, Y. Yang, Enhanced brain targeting of curcumin by intranasal administration of a thermosensitive poloxamer hydrogel, *Journal of Pharmacy & Pharmacology*, 65, 807–816, (2013), doi: 10.1111/jphp.12043.
13. M. Agrawala, S. Saraf, S. Saraf, S.G. Antimisiaris, M.B. Chougule, S.A. Shoyele, A. Alexander, Nose-to-brain drug delivery: An update on clinical challenges and progress towards approval of anti-Alzheimer drugs, *Journal of Controlled Release,* 281, 139-177, (2018), doi: 10.1016/j.jconrel.2018.05.011.
14. R. Scherließ, Nasal formulations for drug administration and characterization of nasal preparations in drug delivery, *Ther Deliv*., 11(3):183-191, (2020), doi: 10.4155/tde-2019-0086.
15. L.A. Keller, O. Merkel, A. Popp, Intranasal drug delivery: opportunities and toxicologic challenges during drug development, *Drug Deliv Transl Res*., 25:1–23, (2021), doi: 10.1007/s13346-020-00891-5.
16. P. Arora, S. Sharma, S. Garg, Permeability issues in nasal drug delivery, *Drug Discovery Today*, 7(18), 967–975, (2002), doi:10.1016/s1359-6446(02)02452-2.
17. F. Bortolotti, A.G. Balducci, F. Sonvico, P. Russo, G. Colombo, *In vitro* permeation of desmopressin across rabbit nasal mucosa from liquid nasal sprays: the enhancing effect of potassium sorbate, *Eur J Pharm Sci*., 37(1):36-42, (2009), doi: 10.1016/j.ejps.2008.12.015.
18. A.G. Balducci, L. Ferraro, F. Bortolotti, C. Nastruzzi, P. Colombo, F. Sonvico, P. Russo, G. Colombo, Antidiuretic effect of desmopressin chimera agglomerates by nasal

administration in rats. *Int J Pharm*., 440(2):154-60, (2013), doi: 10.1016/j.ijpharm.2012.09.049.

19. N. Haffejee, J. Du Plessis, D.G. Müller, C. Schultz, A.F. Kotzé, C. Goosen, Intranasal toxicity of selected absorption enhancers. *Pharmazie*, 56(11):882-8, (2001).
20. G. Rassu, S. Fancello, M. Roldo, M. Malanga, L. Szente, R. Migheli, E. Gavini, P. Giunchedi, Investigation of Cytotoxicity and Cell Uptake of Cationic Beta-Cyclodextrins as Valid Tools in Nasal Delivery, *Pharmaceutics*, 12(7):658, (2020), doi: 10.3390/pharmaceutics12070658.
21. G. Rassu, E. Soddu, M. Cossu, A. Brundu, G. Cerri, N. Marchetti, L. Ferraro, R.F. Regan, P. Giunchedi, E. Gavini, A. Dalpiaz, Solid microparticles based on chitosan or methyl-β-cyclodextrin: A first formulative approach to increase the nose-to-brain transport of deferoxamine mesylate, *Journal of Controlled Release*, 201, 68–77, (2015), doi: 10.1016/j.jconrel.2015.01.025.
22. A.E. Pontiroli, E. Tagliabue, Therapeutic Use of Intranasal Glucagon: Resolution of Hypoglycemia, *Int J Mol Sci*., 20(15):3646, (2019), doi: 10.3390/ijms20153646.
23. K. Manta, P. Papakyriakopoulou, M. Chountoulesi, D. Diamantis, D. Spaneas, V. Vakali, N. Naziris, M.V. Chatziathanasiadou, I. Andreadelis, K. Moschovou, I. Athanasiadou, P. Dallas, D.M. Rekkas, C. Demetzos, G. Colombo, S. Banella, U. Javornik, J. lavec, T. Mavromoustakos, A.G. Tzakos, G. Valsami, Preparation and biophysical characterization of Quercetin inclusion complexes with β-cyclodextrin derivatives for the preparation of possible nose-to-brain Quercetin delivery systems. *Molecular Pharmaceutics*, 17, 11, 4241-4255, (2020), doi: 10.1021/acs.molpharmaceut.0c00672.
24. L. Tiozzo Fasiolo, M.D. Manniello, E. Tratta, F. Buttini, A. Rossi, F. Sonvico, F. Bortolotti, P. Russo, G. Colombo, Opportunity and challenges of nasal powders: Drug formulation and delivery. *Eur J Pharm Sci.*, 113:2-17, (2018), doi: 10.1016/j.ejps.2017.09.027.
25. P. Russo, C. Sacchetti, I. Pasquali, R. Bettini, G. Massimo, P. Colombo, A. Rossi, Primary Microparticles and Agglomerates of Morphine for Nasal Insufflation, *Journal of Pharmaceutical Sciences*, 95(12), 2553–2561, (2006), doi: 10.1002/jps.20604.
26. N. Sanghavi, S.D. Bhosale, Y. Malode. RP-HPLC method development and validation of Quercetin isolated from the plant Tridax procumbens L., *Journal of Scientific and Innovative Research*, 3, 594−597, (2014).
27. L. Tiozzo Fasiolo, M.D. Manniello, F. Bortolotti, F. Buttini, A. Rossi, F. Sonvico, P. Colombo, G. Valsami, G. Colombo, P. Russo, Anti-inflammatory flurbiprofen nasal powders for nose-

575 to-brain delivery in Alzheimer's disease, *Journal of Drug Targeting*, 1–31, (2019),
576 doi.org/10.1080/1061186X.2019.1574300.
577 28. L. Dian, E. Yu, X. Chen, X. Wen, Z. Zhang, L. Qin, Q. Wang, G. Li, C. Wu, Enhancing oral
578 bioavailability of quercetin using novel soluplus polymeric micelles, *Nanoscale Research*
579 *Letters*, 9 (1):2406, (2014), doi: 10.1186/1556-276X-9-684.
580 29. P. Mahalapbutr, P. Wonganan, T. Charoenwongpaiboon, M. Prousoontorn, W. Chavasiri,
581 T. Rungrotmongkol, Enhanced Solubility and Anticancer Potential of Mansonone G By β-
582 Cyclodextrin-Based Host-Guest Complexation: A Computational and Experimental Study,
583 *Biomolecules*, 9, 545, (2019), doi: 10.3390/biom9100545.
584 30. D.R. De Araujo, S.S. Tsuneda, C.M.S. Cereda, F. Del G.F. Carvalho, P.S.C. Preté, S.A.
585 Fernandes, F. Yokaichiyac, M.K.K.D. Francoc, I. Mazzaroc, L.F. Fraceto, A. de F.A. Braga, E.
586 de Paula, Development and pharmacological evaluation of ropivacaine-2-hydroxypropyl-
587 β-cyclodextrin inclusion complex, *European Journal of Pharmaceutical Sciences*, 33(1),
588 60–71, (2008), doi:10.1016/j.ejps.2007.09.010.
589 31. I. Uchegbu, Z. Wang, G. Xiong, A. Tsang, A. Schatzlein, Nose to brain delivery, *Journal of*
590 *Pharmacology and Experimental Therapeutics*, jpet.119.258152., (2019),
591 doi:10.1124/jpet.119.258152.
592 32. Ng. Shiow-Fern, J. Rouse, D. Sanderson, G. Eccleston, A Comparative Study of
593 Transmembrane Diffusion and Permeation of Ibuprofen across Synthetic Membranes
594 Using Franz Diffusion Cells, *Pharmaceutics*, 2(2), 209–223, **(**2010),
595 doi:10.3390/pharmaceutics2020209.
596 33. A. Giuliani, A.G. Balducci, E. Zironi, G. Colombo, F. Bortolotti, L. Lorenzini, V. Galligioni, G.
597 Pagliuca, A. Scagliarini, L. Calzà, F. Sonvico, *In vivo* nose-to-brain delivery of the
598 hydrophilic antiviral ribavirin by microparticle agglomerates, *Drug Deliv*., ,25(1):376-387,
599 (2018), doi: 10.1080/10717544.2018.
600 34. T. Loftsson, Drug permeation through biomembranes: cyclodextrins and the unstirred
601 water layer*, Die Pharmazie - An International Journal of Pharmaceutical Sciences*, Volume
602 67, Number 5, pp. 363-370(8), (2012).
603 35. B. Steffansen, B. Brodin, C.U. Nielsen, Passive diffusion of drug substances: The concepts
604 of flux and permeability. *Molecular biopharmaceutics: Aspects of drug characterization,*
605 *drug delivery and dosage form evaluation,* Pharmaceutical Press, (2010).
606 36. P. Liu, O. De Wulf, J. Laru, T. Heikkilä, B. van Veen, J. Kiesvaara, J. Hirvonen, L. Peltonen,
607 T. Laaksonen, Dissolution Studies of Poorly Soluble Drug Nanosuspensions in Non-sink

608 Conditions. *AAPS PharmSciTech*, 14(2), 748–756, (2013), doi:10.1208/s12249-013-9960-
609 2.
610 37. S. Zsikó , E. Csányi , A. Kovács, M. Budai-Szucs, A. Gácsi and S. Berkó, Methods to Evaluate
611 Skin Penetration *In Vitro*. Scientia Pharmaceutica 87, 19-21, (2019),
612 doi:10.3390/scipharm87030019
613 38. Y. Mitsunaga, H. Takanaga, H. Matsuo, M. Naito, T. Tsuruo, H. Ohtani, Y. Sawada. Effect
614 of bioflavonoids on vincristine transport across blood-brain barrier. *Eur J Pharmacol*.,
615 395: 193–201, (2000).
616 39. Achim G. Beule. Physiology and pathophysiology of respiratory mucosa of the nose and
617 the paranasal sinuses.GMS *Curr Top Otorhinolaryngol Head Neck Surg*., (2011), doi:
618 10.3205/cto000071.
619 40. L.X. Yu, G.L. Amidon, J.E. Polli, H. Zhao, M.U. Mehta, D.P. Conner, V.P. Shah, L.J. Lesko,
620 M.L. Chen, V.H.L. Lee, A.S. Hussain, *Pharmaceutical Research*, 19(7), 921–925, (2002),
621 doi:10.1023/a:1016473601633.
622 41. A. Jaipal, M.M. Pandey, S.Y. Charde, P.P. Raut, K.V. Prasanth, R.G. Prasad, Effect of HPMC
623 and mannitol on drug release and bioadhesion behavior of buccal discs of buspirone
624 hydrochloride: In-vitro and in-vivo pharmacokinetic studies, *Saudi Pharmaceutical*
625 *Journal*, 23(3), 315–326, (2015), doi:10.1016/j.jsps.2014.11.012.

626 **Figure Captions**

627 **Figure 1.** Normalized X-Ray diffractograms of: (A) quercetin (Que), Me-β-CD and formulations
628 F1-F4, (B) quercetin (Que), HP-β-CD and formulations F5-F8.

629 **Figure 2.** SEM images of (A) Que, (B) MLMPs , (C) Me-β-CD, (D) HP-β-CD, (E) Que-Me-β-CD
630 (F1), (F) Que-Me-β-CD:MLMPs (75:25) (F2), (G) Que-Me-β-CD:MLMPs (50:50) (F3), (H) Que-
631 Me-β-CD:MLMPs (25:75) (F4), (I) Que-HP-β-CD (F5), (J) Que-HP-β-CD:MLMPs (75:25) (F6), (K)
632 Que-HP-β-CD:MLMPs (50:50) (F7), and (L) Que-HP-β-CD:MLMPs (25:75) (F8). A, B, C, D, E, I at
633 x1000 magnification and F, G, H, J, K, L at x3000 magnification.

634 **Figure 3.** Permeation profiles through regenerated cellulose membranes for formulations F1-
635 F4 (A), F5-F8 (B) and pure Que (A, B), expressed as % of loading dose (mean ± SD, n= 3).

636 **Figure 4.** Permeation profiles through regenerated cellulose membranes for formulations F1-
637 F8 and pure Que, expressed as quantity permeated per unit area (mean ± SD, n=3).

638 **Figure 5.** Permeation profiles through rabbit nasal mucosa for formulations F1-F4 (A), F5-F8
639 (B) and pure Que (A, B), expressed as % of loading dose (mean ± SE, n= 5).

640 **Figure 6.** Permeation profiles through rabbit nasal mucosa for formulations F1-F8, expressed
641 as quantity permeated per unit area (mean ± SE) Vs time.

642 **Table 1.** Que and CD content in the prepared formulations

	Formulation	Complex:MLMPs	Que content	
			% w/w	Amount (mg) in 25 mg of F ± SD
Que-Me-β-CD	F1	100:0	12.4 ± 0.719	3.1 ± 0.17
	F2	75:25	8.6 ± 0.14	2.1 ± 0.04
	F3	50:50	6.3 ± 0.04	1.56 ± 0.009
	F4	25:75	3.0 ± 0.02	0.74 ± 0.26
Que-HP-β-CD	F5	100:0	7.3 ± 0.15	1.8 ± 0.04
	F6	75:25	5.5 ± 0.03	1.38 ± 0.006
	F7	50:50	3.8 ± 0.01	0.943 ± 0.003
	F8	25:75	1.8 ± 0.03	0.454 ± 0.008

643 Que: Quercetin, CD: Cyclodextrin, Que-Me-β-CD: Quercetin-Methyl-β-Cyclodextrin, Que-HP-β-CD:
644 Quercetin-Hydroxypropyl-β-Cyclodextrin, MLMPs: Mannitol/Lecithin microparticles, F: formulation

645 **Table 2.** Regression analysis of the amount of Que permeated per unit area vs time for formulations
646 F1-F8.

	Formulation (F)*	Slope	Intercept	R^2
Que-Me-β-CD	F1	0.0014 ± 0.00005	0.0034 ± 0.0038	0.996 ± 0.005
	F2	0.0009 ± 0.00008	0.0084 ± 0.0055	0.977 ± 0.009
	F3	0.0006 ± 0.00002	-0.0022 ± 0.0016	0.995 ± 0.003
	F4	0.0002 ± 0.00001	0.0009 ± 0.0007	0.990 ± 0.001
Que-HP-β-CD	F5	0.0018 ± 0.00006	-0.0058 ± 0.0046	0.998 ± 0.006
	F6	0.0012 ± 0.0001	0.0079 ± 0.0075	0.975 ± 0.012
	F7	0.0009 ± 0.00007	-0.0038 ± 0.005	0.975 ± 0.009
	F8	0.0003 ± 0.00001	0.0004 ± 0.0008	0.9951 ± 0.0013

647 *Formulations contain MLMPs (mannitol/lecithin microparticles) at a ratio with Que-Me-β-CD (F1-F4)
648 or Que-HP-β-CD (F5-F8) complex of 0:100, 25:75, 50:50 and 75:25 respectively.

HELLENIC REPUBLIC
National and Kapodistrian University of Athens

School of Health Sciences
Department of Pharmacy
Section of Pharmaceutical Technology

G. Valsami, Professor
e-mail: valsami@pharm.uoa.gr
Tel.: +302107274022
Fax: +302107274027

To the Editor of
The International Journal of Pharmaceutics

Athens 19.04.21

Dear Editor,

We would like to submit this manuscript under the title: "Nasal powders of quercetin-β-cyclodextrin derivatives complexes with mannitol/lecithin microparticles for Nose-to-Brain delivery: In vitro and ex vivo evaluation", to be considered for publication in the International Journal of Pharmaceutics.
In this study, aiming to increase quercetin's disposition into the brain, we prepared nasal powders consisting of quercetin-cyclodextrins lyophilizates blended with spray-dried microparticles of mannitol/lecithin. The solubility of quercetin was increased, while the powders exhibited improved morphological characteristics as observed by X-ray Diffraction and Scanning Electron Microscopy analyses. Further *in vitro* and *ex vivo* characterization using Franz diffusion cells, revealed rapid dissolution and *ex vivo* transport of quercetin across rabbit nasal mucosa, constituting promising results for further evaluation of the *in vivo* performance of the powders after nasal administration and possible nose-to brain delivery of quercetin.
To the best of our knowledge this is the first study investigating the formulation of quercetin-cyclodextrins lyophilizates in nasal powders as candidates for nose-to-brain delivery.

This manuscript is a unique submission and is not being considered for publication elsewhere.

All authors declare no conflict of interest.

Thank you for your time and consideration of our manuscript for publication.
We look forward to hearing from you soon.
Sincerely

Georgia Valsami, PhD
Professor of Biopharmaceutics & Pharmacokinetics

P.S. All authors have read and approved this version of the article, and no part of this paper has been published nor is it submitted for publication elsewhere and will not be submitted elsewhere.

Graphical Abstract (for review)

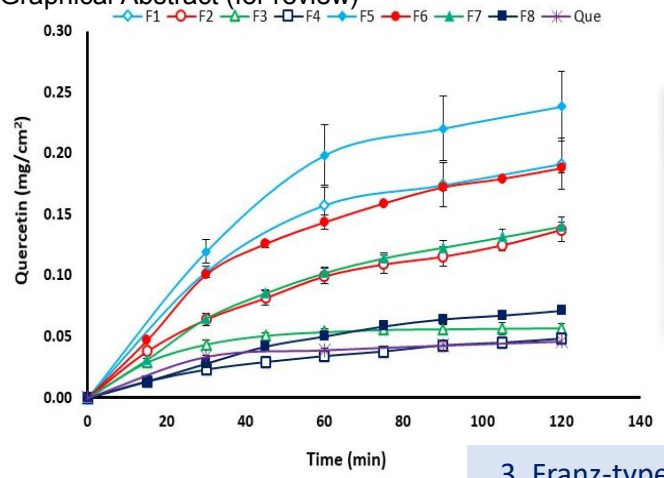

In vitro

1. Lyophilization

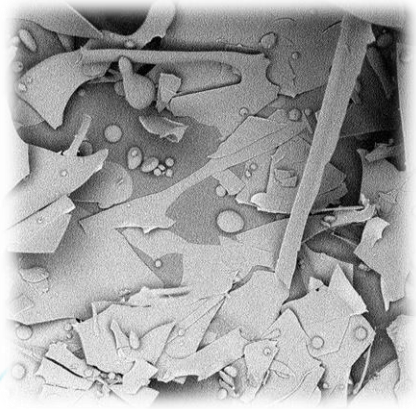

Quercetin-Methyl-β-Cyclodextrin

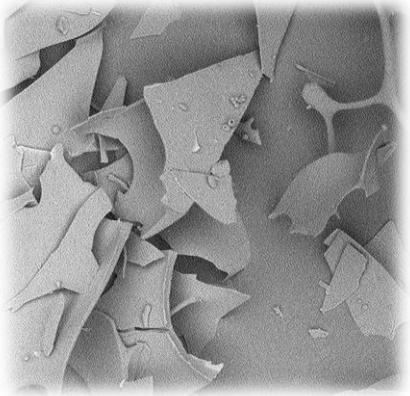

Quercetin-Hydroxypropyl-β-Cyclodextrin

3. Franz-type vertical diffusion cells

Nasal mucosa extraction

Ex vivo

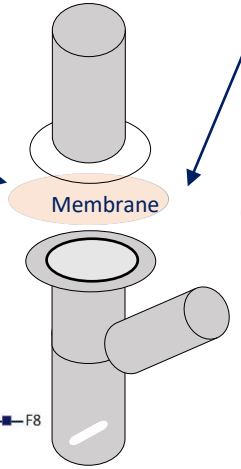

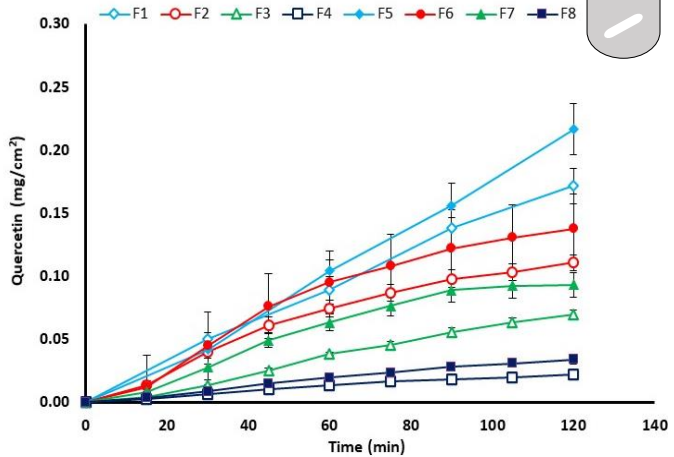

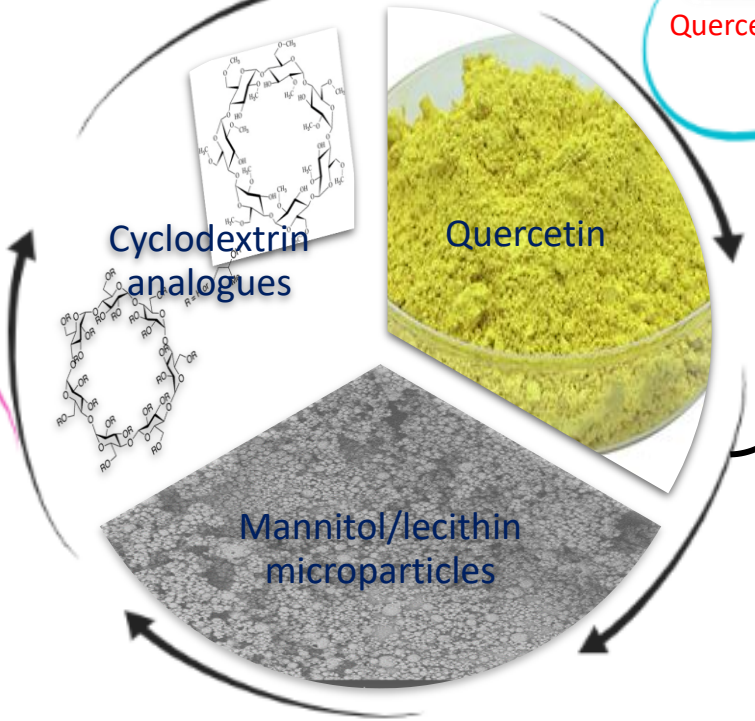

2. Blends of microparticles with lyophilized powders

Blended

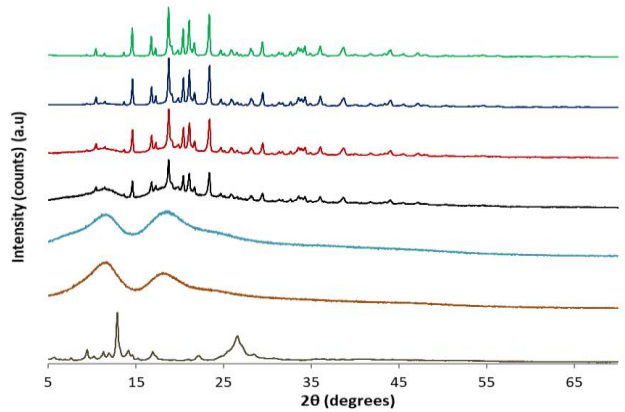

XRD Analysis

Declaration of interests

☒ The authors declare that they have no known competing financial interests or personal relationships that could have appeared to influence the work reported in this paper.

☐The authors declare the following financial interests/personal relationships which may be considered as potential competing interests:

Figure(s)

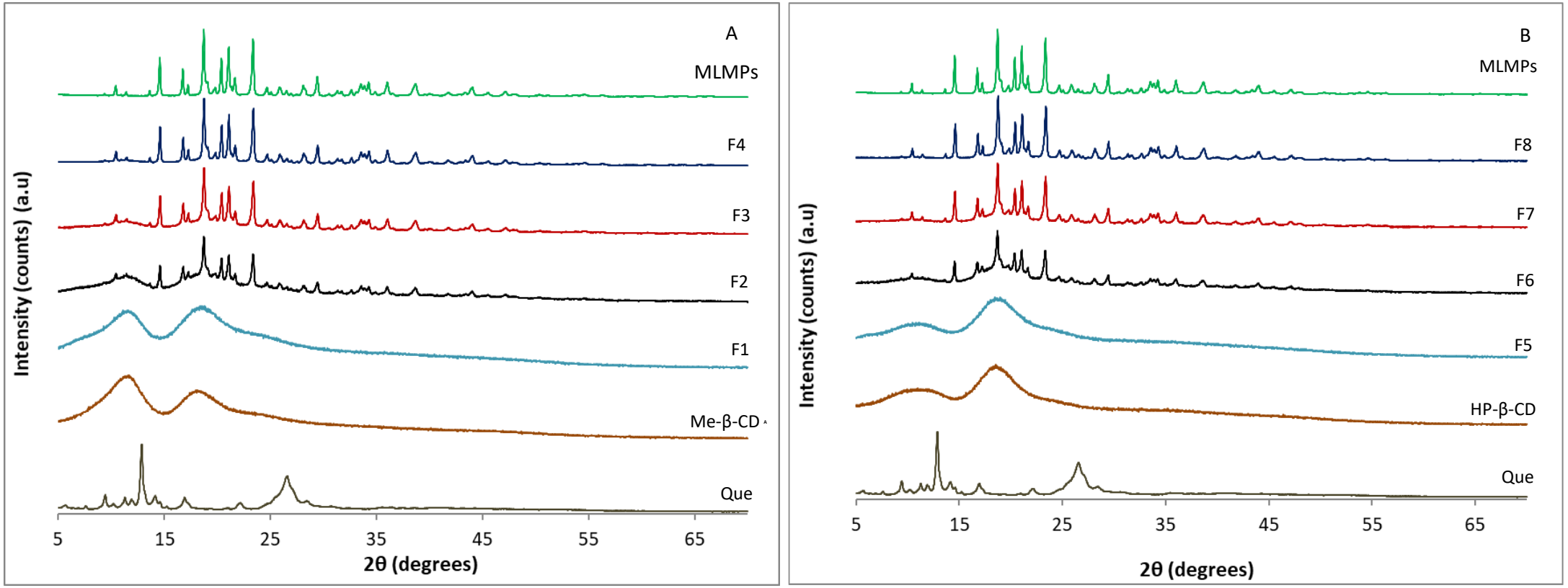

Figure 1. Normalized X-Ray diffractograms of: (A) quercetin (Que), Me-β-CD and formulations F1-F4, (B) quercetin (Que), HP-β-CD and formulations F5-F8.

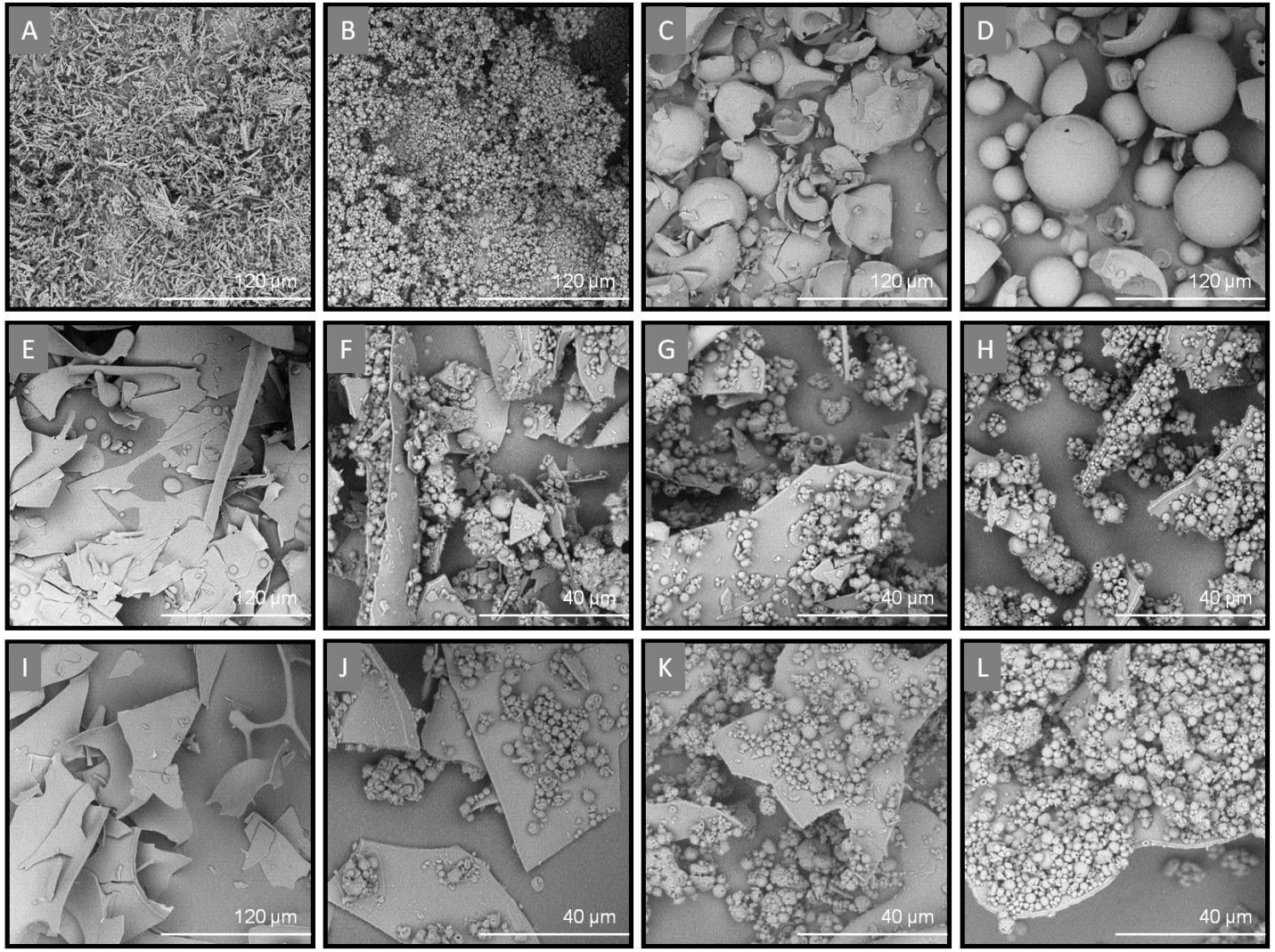

Figure 2. SEM images of (A) Que, (B) MLMPs , (C) Me-β-CD, (D) HP-β-CD, (E) Que-Me-β-CD (F1), (F) Que-Me-β-CD:MLMPs (75:25) (F2), (G) Que-Me-β-CD:MLMPs (50:50) (F3), (H) Que-Me-β-CD:MLMPs (25:75) (F4), (I) Que-HP-β-CD (F5), (J) Que-HP-β-CD:MLMPs (75:25) (F6), (K) Que-HP-β-CD:MLMPs (50:50) (F7), and (L) Que-HP-β-CD:MLMPs (25:75) (F8). A, B, C, D, E, I at x1000 magnification and F, G, H, J, K, L at x3000 magnification.

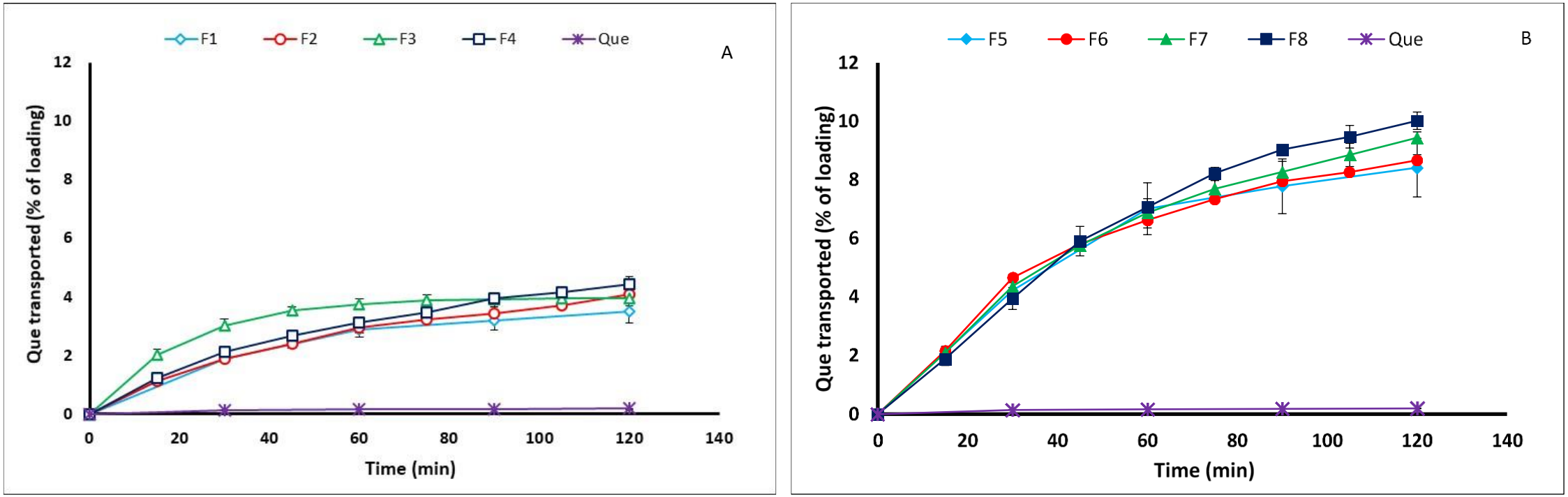

Figure 3. Permeation profiles through regenerated cellulose membranes for formulations F1-F4 (A), F5-F8 (B) and pure Que (A, B), expressed as % of loading dose (mean ± SD, n= 3).

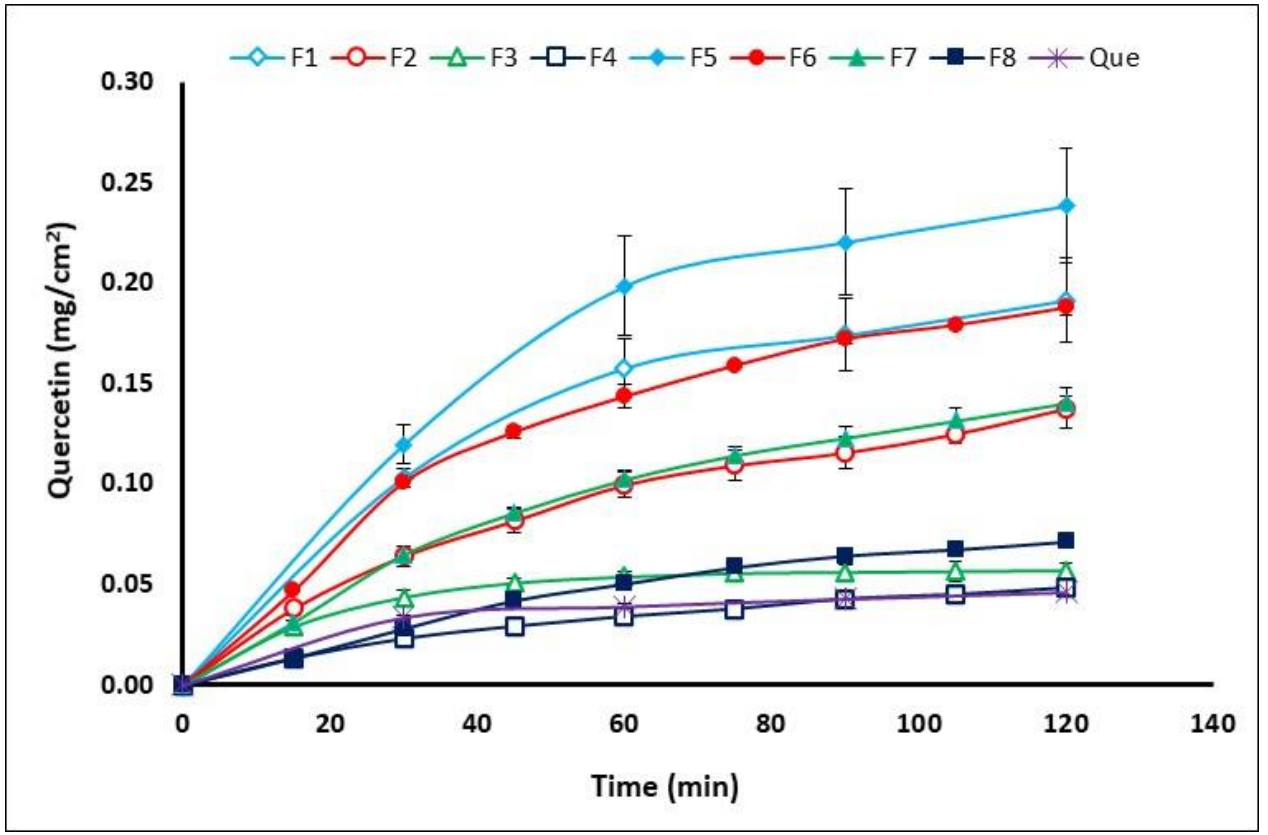

Figure 4. Permeation profiles through regenerated cellulose membranes for formulations F1-F8 and pure Que, expressed as quantity permeated per unit area (mean ± SD, n=3).

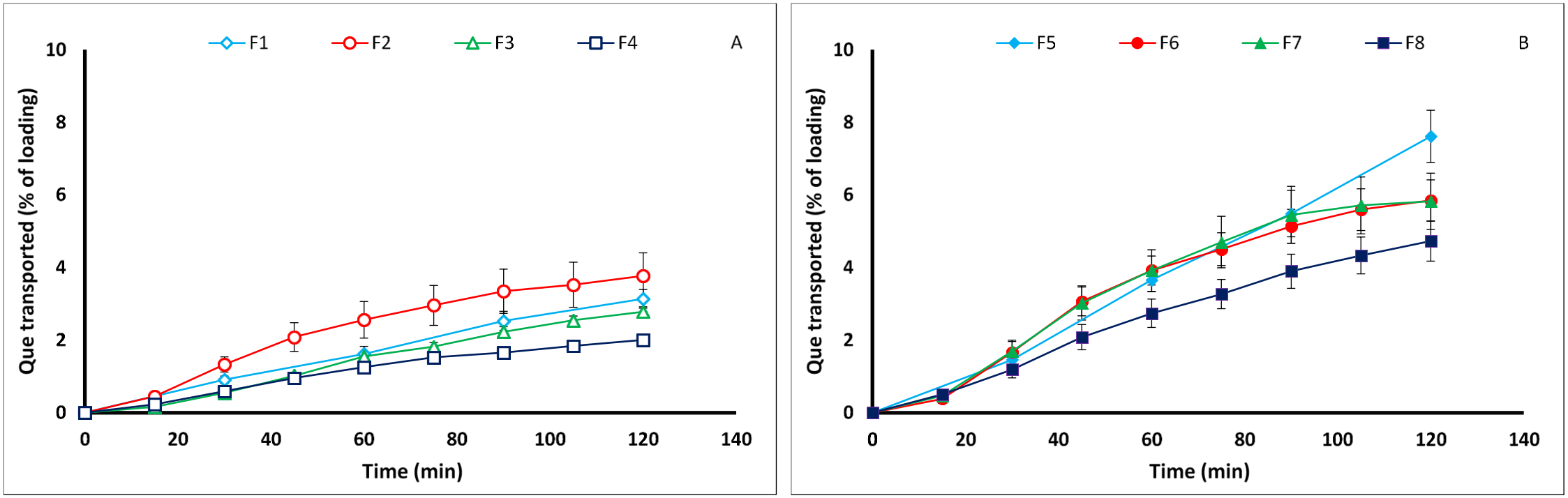

Figure 5. Permeation profiles through rabbit nasal mucosa for formulations F1-F4 (A), F5-F8 (B) and pure Que (A, B), expressed as % of loading dose (mean ± SE, n= 5).

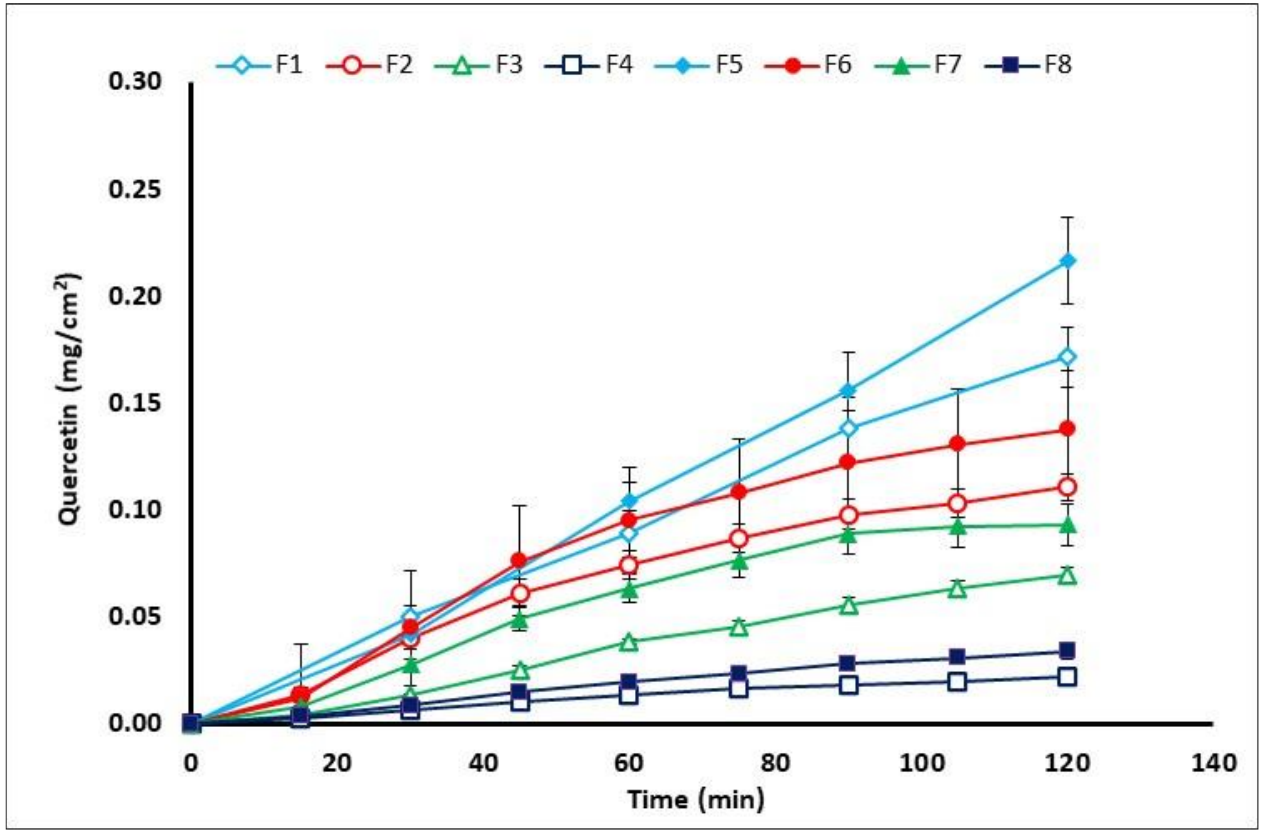

Figure 6. Permeation profiles through rabbit nasal mucosa for formulations F1-F8, expressed as quantity permeated per unit area (mean ± SE) Vs time.